Optical metrology alignment and impact on the measurement performance of the LISA

Technology Package

Optical metrology alignment and impact on the measurement performance of the LISA Technology Package

M Hirth[1], W Fichter[1], N Brandt[1,2], A Schleicher[2], D Gerardi[1,2] and G Wanner[3]

[1] iFR, Universitaet Stuttgart, Pfaffenwaldring 7a, 70569 Stuttgart, Germany
[2] Astrium GmbH, 88039 Friedrichshafen, Germany
[3] Albert Einstein Institut, Callinstrasse 38, 30167 Hannover, Germany

E-mail: `marc.hirth@ifr.uni-stuttgart.de`

Abstract. Aside from LISA Pathfinder's top-level acceleration requirement, there is a stringent independent requirement for the accuracy of the optical metrology system. In case of a perfectly aligned metrology system (optical bench and test masses) it should rather be independent of residual displacement jitter due to control. However, this ideal case will not be achieved as mechanical tolerances and uncertainties lead to a direct impact of test mass and spacecraft displacement jitter on the optical measurement accuracy.

In this paper, we present a strategy how to cover these effects for a systematic requirement breakdown. We use a simplified nonlinear geometrical model for the differential distance measurement of the test masses which is linearized and linked to the equations of motion for both the spacecraft and the two test masses. This leads from test mass relative displacement to a formulation in terms of applied force/torque and thus allows to distinguish the absolute motion of each of the three bodies. It further shows how motions in each degree of freedom couple linearly into the optical measurement via DC misalignments of the laser beam and the test masses. This finally allows for deriving requirements on the alignment accuracy of components and on permittable closed-loop acceleration noise.

In the last part a budget for the expected measurement performance is compiled from simulations as no measurement data is available yet.

1. Measurement model

The configuration of the two test masses (TMs) and the optical bench (OB) for LISA Pathfinder is shown in figure 1. Whenever the TM x-faces and the optical metrology system (OMS) are not nominally aligned, the differential distance measurement Δx along the sensitive axis may be degraded due to coupling of residual control jitter in other degrees of freedom into the sensitive axis. That means that DC misalignments in position and attitude of the TMs and the laser beams couple linearly via linear and angular displacement noise of either TMs or the spacecraft (SC).

To gain insight into this issue a measurement model for the differential distance readout of the two TMs was derived. This model does not aim for an exact description of the distance measurement of the laser beam as the whole optical bench setup would have to be taken into account. It rather describes the distance between the laser beam reflection points on the x-faces

of the TMs. The measurement direction of this model is the x-axis of the OB frame, i.e. the connecting line between the nominal center of mass (CoM) positions of the two TMs.

Besides the OB frame, additional coordinate frames were introduced. The XMRFi frame serves as reference frame on the reflecting surface of TM i (i=1,2). Its origin is defined as the intersection of the reflecting surface and its normal passing through the CoM of the respective TM, the x-axis is aligned with this normal. The RPFi origins are located at the laser beam reflection points on each TM with all axes aligned to the so-called interferometer axis frame (IAFi). The origin of the latter lies in the as-built reflection point on the dummy TM with the x-axis along the angle bisector of the as-built incident and reflected laser beams when differential wave front sensing (DWS) senses zero angles. For all these frames positive axes directions are defined 'along' OB frame axes. Figure 1 depicts the frames and notations in use exemplary for the xy-plane.
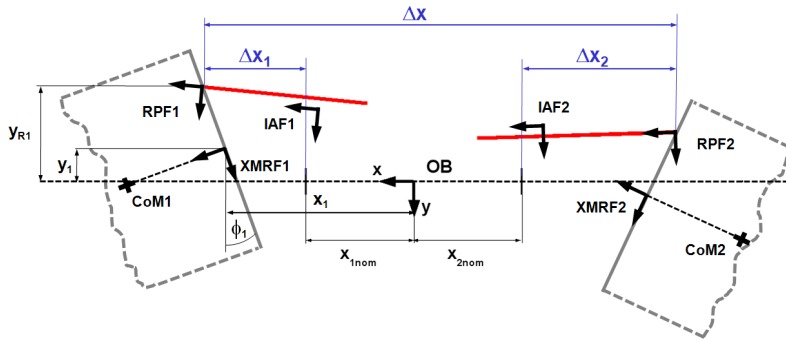

Figure 1. Coordinate frames and notations used in the measurement model, x_{1nom} and x_{2nom} are the nominal distances between the XMRF frames and the OB frame

For ideally aligned x-faces (i.e. $\phi_i = 0$) the measurement would obviously be the desired measurement $\Delta x = x_1 - x_2$ which is simply the distance between the known XMRFi frames on the TM faces. However, angular misalignments of the TMs additionally contribute to Δx if the reflection points do not correspond with the XMRFi frames. The final measurement equation can be written as:

$$
\begin{aligned}
\Delta x &= b_{x1}x_1 + b_{x2}x_2 - (y_{R1} - y_1)\phi_1 + (y_{R2} - y_2)\phi_2 + (z_{R1} - z_1)\eta_1 - (z_{R2} - z_2)\eta_2 \\
&\quad + b_{\phi_1^2}\phi_1^2 + b_{\phi_2^2}\phi_2^2 + b_{\eta_1^2}\eta_1^2 + b_{\eta_2^2}\eta_2^2
\end{aligned} \tag{1}
$$

In order to account for quadratic terms in angles and for the non-ideal sensitivity of the interferometer readout (which is not resolvable with the simple geometrical model) an additional set of model parameters b_j was introduced. The relevant parameters can be extracted from complex alignment simulations that take into account the complete setup of all optical elements and properties of the laser beam.

Generally each XMRF coordinate in the measurement equation may comprise a DC and a noise component, e.g. $y_1 = y_1^{DC} + \bar{y}_1$. Thus, it is possible to rewrite equation (1) with all coordinates separated into terms linear in DC and displacement noise and quadratic terms in DC or displacement noise. All quadratic terms can be neglected as on the one hand pure DC terms do not introduce additional errors in the measurement bandwidth and on the other hand - as the DC components are much larger than the noise contributions - quadratic terms in noise have no driving impact. The remaining expression is linear in noise and can be written in vector form:

$$
\Delta x = \mathbf{v}_1^T \mathbf{r}_1 + \mathbf{w}_1^T \boldsymbol{\varphi}_1 + \mathbf{v}_2^T \mathbf{r}_2 + \mathbf{w}_2^T \boldsymbol{\varphi}_2 \tag{2}
$$

where $\mathbf{r}_i$ and $\boldsymbol{\varphi}_i$ are the position (x,y,z) and attitude (θ,η,ϕ) noise components relative to OB frame while the DC position and attitude alignments are arranged in the vectors $\mathbf{v}_i$ and $\mathbf{w}_i$. This equation shows how displacement noise relative to the OB frame couples via DC alignments of the TM x-faces into the differential distance measurement.

2. Relative vs. absolute coordinates

From equation (2) it is obvious that if the measurement error should be kept below an appropriate overall requirement, both DC misalignments and displacement noise have to be bounded. While the first directly leads to design requirements for OB, TMs and interfaces, the latter is related to requirements on control. In case of LISA Pathfinder, control is subdivided in attitude, drag-free and suspension loops [1]. Attitude and drag-free control is performed using colloid thrusters or FEEPs while suspension control acts directly on the TMs using electrostatic forces and torques. In addition, different "external" noise sources (i.e. not due to actuation) act on the SC and each TM and different readout noise is present in the signals of the sensors in use for each loop. With a description in terms of relative coordinates as in equation (2) it is impossible to distinguish whether displacement noise is induced by force noise on the TM or on the SC and thus how control has to be improved to mitigate the impact on the measurement accuracy. As a consequence it is necessary to separate the relative motion into absolute motion of SC/OB and the two TMs.

This separation is done by replacing the relative TM coordinates with the relations for the relative TM motion that come from the linearized equations of motion [3]. These are modified such that SC and TM CoMs are replaced by the OB and XMRF origins respectively. Similar to the relative coordinates in equation (1) acceleration terms (i.e. applied forces/torques per unit mass) in the equations of motion contain DC and noise components. Again only noise components in the measurement bandwidth are of interest and DC contributions are neglected. Substitution into the measurement model finally gives another equation which is linear in noise:

$$\Delta\ddot{x} = \mathbf{C}_{DC}^{T} \begin{bmatrix} \mathbf{a}_{OB} \\ \boldsymbol{\alpha}_{OB} \\ \mathbf{a}_{TM1} \\ \boldsymbol{\alpha}_{TM1} \\ \mathbf{a}_{TM2} \\ \boldsymbol{\alpha}_{TM2} \end{bmatrix} \tag{3}$$

where the vector $\mathbf{C}_{DC}$ summarizes all misalignment contributions that couple with linear and angular closed-loop acceleration noise $\mathbf{a}$ or $\boldsymbol{\alpha}$ in the 18 OB (i.e. SC) and TM degrees of freedom. A detailed description of the involved terms can be found in [2].

3. Requirement breakdown strategy

Given the alignment vector $\mathbf{C}_{DC}$ from equation (3), requirements can be allocated to the magnitude of each row, i.e. the sum of all misalignment terms that couple with noise in one degree of freedom. Subsequently, this total is broken down to the single contributions of each entry. The resulting requirements can generally be assigned to three groups: requirements on the inertial sensor design (e.g. TM surface non-orthogonality), on the OMS design (IAF-alignments, readout sensitivities and DWS sensing bias) and requirements on the final integrated OMS-TM system (XMRF-IAF relations). The first two groups represent fixed systems (pre-flight) whereas the latter remains adjustable to some extent due to control during operation. Now as requirements on the alignment accuracy are available (in the range of some tens of μm or μrad), requirements on the acceleration noise can be derived from the top-level requirement on the measurement error which is given as $\sqrt{S_{\Delta x, req}} = 6$ pm/$\sqrt{\text{Hz}}$ at 30 mHz (the frequency shape is shown in figure 2). As it is given in terms of a spectral density, the differential distance readout error equation (3) has to be converted using:

$$S_{\Delta\ddot{x}} = \mathbf{C}_{DC}^{T} \mathbf{S}_a \mathbf{C}_{DC} = (2\pi f)^4 S_{\Delta x} \tag{4}$$

In this general form, $\mathbf{S_a}$ denotes the spectral density matrix of the acceleration noise in the considered 18 degrees of freedom. For the breakdown of requirements on acceleration noise it

is assumed that - even if the different DoF will be coupled to some extent due to control - all noise contributions are uncorrelated. Then above equation collapses to

$$S_{\Delta x} = \frac{1}{(2\pi f)^4} \sum_{j=1}^{18} C_{DC,j}^2 S_{a_j} = \frac{1}{(2\pi f)^4} \sum_{j=1}^{18} S_{\Delta \ddot{x}_j} = \sum_{j=1}^{18} S_{\Delta x_j} \qquad (5)$$

where S_{a_j} denote the auto-spectra of the acceleration noise in each degree of freedom, i.e. the main diagonal elements of $\mathbf{S}_a$. This assumption allows a direct apportioning of the total $S_{\Delta x,req}$ to each $S_{\Delta x_j}$ that comes from a coupling with a (non-zero) misalignment component $C_{DC,j}$. Then, according to equation (5) requirements on single acceleration noise terms can be derived using the magnitude of the respective alignment requirement on $C_{DC,j}$.

Preliminary investigations using the requirement values for the misalignments and acceleration noise data from a LTP closed-loop frequency analysis revealed that $S_{\Delta x_j}$ contributions that come from SC acceleration noise have a driving impact and the individual requirements could not be met over the whole measurement bandwidth. This mainly thruster-induced noise led to a redesign of the drag-free loops (that use the FEEPs as actuators) including the additional requirements from the alignment coupling. As DFACS uses specific control coordinates (i.e. the SC is controlled w.r.t. selected TM DoF [1]), above decomposition into OB and TM acceleration noise is not directly applicable to derive control requirements. The strategy and results for the successful loop redesign was shown in [4].

4. Performance results

As no measurements are available all relevant information for a performance budget is extracted from models. As mentioned above, acceleration noise data comes from a closed-loop frequency domain model of LISA Pathfinder implemented in *Matlab*. From this model we get:

$$\mathbf{S}_a(f) = \mathbf{H}^{*T}(f) \mathbf{S}_n(f) \mathbf{H}(f). \qquad (6)$$

Here $\mathbf{H}$ is the matrix of the frequency response functions of the closed loop system ($\mathbf{H}^{*T}$ denotes its complex conjugate transpose) and $\mathbf{S}_n$ is the spectral density matrix of the noise sources under consideration. These are thruster (FEEP) noise, star tracker noise, capacitive actuation/readout noise and internal readout noise of the optical metrology system. $\mathbf{S}_n$ is modeled as uncorrelated white noise input with magnitude one, noise scaling and noise shape is already included in the frequency response functions.

Including measurement data into the budget will not be possible for the entire set of misalignment terms as they partially depend on the real in-flight orientation and position of the TMs. For orthogonality of the TMs and OB flight model properties, no data exists yet but will be available before launch. As an intermediate stage, alignments are taken that come from a simulation of the OB bonding procedure and the in-flight alignment of the TMs carried out the Albert Einstein Institute [5].

They use a $C++$ program to set up position and attitude of the single optical elements on the OB. This setup may represent the nominal bench or a misaligned layout. The latter is obtained by placing the optical bench elements and dummy test masses one after another (according to the OB alignment plan) randomly within their expected tolerance range. Clipped normal distributions are employed to generate this random positioning. In a second step the Fortran program *OptoCad* is used to trace the laser beams through the optical setup. It allows for computing beam parameters (at desired positions), reflection points and incident angles on optical elements taking into account their refractive indices. Finally a third C program derives the photodiode signals of each interferometer using similar routines as implemented in the data

management unit.

As mentioned above the sequence for the setup of the misaligned bench is chosen in a way that it represents the strategy of how the real elements on the bench will be bonded. Afterwards the dummy TMs are replaced by the 'real' TMs for which the in-flight alignment procedure is simulated, i.e. the TMs are rotated until 'DWS zero' condition is reached (IAFs/RPFs coincide with XMRFs). The whole procedure is carried out as Monte Carlo simulation (>4000 runs). Combining the data of frequency analysis and alignment simulation, it is possible to
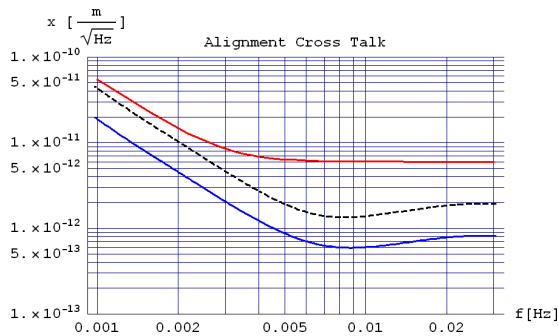

Figure 2. Performance results gained from Monte Carlo simulation data for misalignments and noise from closed-loop frequency domain analysis. Lines in plot are:

—— Requirement

—— RMS

– – – Mean+3σ

compute the misalignment-induced measurement error $\sqrt{S_{\Delta x}}$ according to equation (4). This was done for all Monte Carlo runs and the result is shown in Fig. 2. Concerning the RMS of all performance results the top level requirement can safely be met with large margin. If the 3σ-curve is considered as representative worst case, still a factor of about 3 is available at the upper end of the measurement bandwidth of 30mHz. Towards lower frequencies the margin decreases but still remains at about 25%.

It should be noted here that the performance results do not account for possible improvements due to any kind of calibration procedure using known misalignment values.

5. Correlation of acceleration noise

For the requirement breakdown, it was assumed that the acceleration noise contributions are uncorrelated, i.e. the non-diagonal elements of $\mathbf{S_a}$ are zero to allow the application of equation (5). However, the spectral density matrix $\mathbf{S_a}$ computed for the closed loop system is not purely diagonal. Thus, for an exact breakdown of $\sqrt{S_{\Delta x}}$ also the cross spectra of $\mathbf{S_a}$ would have to be considered. To estimate the error due to this neglection, the relative difference between both results is investigated:

$$\Delta = \left(\sqrt{S_{\Delta x,uc}} - \sqrt{S_{\Delta x,real}} \right) / \sqrt{S_{\Delta x,uc}} \qquad (7)$$

Here $\sqrt{S_{\Delta x,uc}}$ denotes the simplified result of equation (5) while $\sqrt{S_{\Delta x,real}}$ gives the real contribution from equation (4). For $\Delta < 0$ the real performance is worse than predicted from the uncorrelated model. As the results are highly dependent on the magnitude and signs of the underlying alignment combinations, we use all data of the AEI Monte Carlo simulation for the comparison. The black set of lines in figure 3 show the Δ of each run, the red line represents the respective mean difference of all runs. The upper bound of the relative difference is approximately +30% at very low frequency and +25% at about 10 mHz. Thus, in best case the measurement error is overestimated up to these levels. This would even allow a relaxation of the single axes acceleration noise requirements. The lower bound varies down to about -20% around 10 mHz and results to an underestimation of the measurement error. In these cases the cross-spectra contributions would lead to more stringent requirements on acceleration noise. However, the mean difference over all runs remains below 5% over the whole measurement bandwidth.
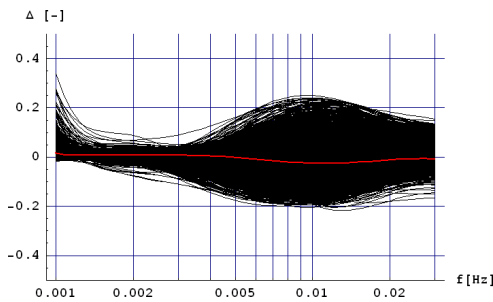
Figure 3. Relative difference (noise in OB coordinates), red line represents mean
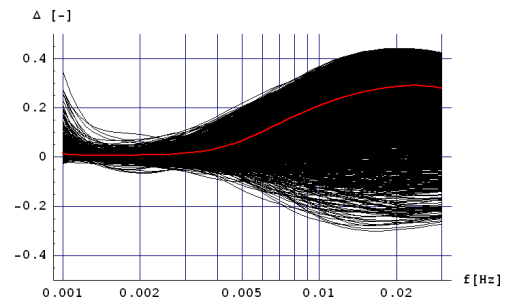

Figure 4. Relative difference (noise in DF coordinates), red line represents mean

This makes the applied breakdown strategy and lower level requirements on $\sqrt{S_{a_j}}$ safely applicable. Even more if it is kept in mind that the expected overall performance contains enough margin to the top-level requirement, see figure 2.

As additional controller requirements were derived for drag-free coordinates, the same investigation was carried out for drag-free rather than OB coordinates, see figure 4. At low frequencies the situation is similar. However for higher frequencies there is a larger spread in Δ, ranging from about -30% to 45%. In particular, the mean is no longer around zero, but raises up to about 30% at high frequencies. Though this is still not critical for the noise budget as the impact on the real performance is overestimated compared and the derived acceleration noise requirements on DF-axes tend to be conservative. The wider spread in Δ using the drag-free axes description was expectable: Angular motion of the OB gets directly mapped into lateral motion of two DF-axes (e.g. ϕ-motion into y_1 and y_2), thus the same noise source is obviously present on multiple axes and increases correlation. This also arises from the following:

For both DF and OB coordinate description the main contributors to the relative difference are FEEP noise (at frequencies larger 3 mHz) and star tracker noise (at very low frequencies). If these noise sources (both related to SC motion) are intentionally removed from the system, figures 3 and 4 become nearly identical (with nearly zero mean and $|\Delta|$ well below 20% for all frequencies).

6. Conclusion

In this paper it was presented how misalignments between the OMS and the inertial sensor of LISA Pathfinder that degrade the differential distance measurement of LISA Pathfinder can be covered using a simple nonlinear measurement model. Moreover it was depicted how the requirement on the measurement error could be broken down into different alignment and noise requirements. A strategy was shown how to separate the measurement errors due to noise inducing TM displacements from noise inducing SC displacement. The latter was identified as driver of misalignment effects and led to a redesign of the drag-free loops.

Subsequently a budget was presented that includes the noise performance of the updated controller design and Monte Carlo simulation data of the expected misalignments from a complex optical model. The results showed that measurement error is likely to be well below the requirement over the whole measurement bandwidth. Finally, it was shown that the assumption of uncorrelated acceleration noise in all degrees of freedom that was used for the requirement breakdown is no significant misjudgement and derived requirements can properly be used.

References

[1] Fichter W, Schleicher A and Vitale S 2007 *Lasers, Clocks and Drag-Free*, ed H Dittus, C Laemmerzahl et al (Berlin: Springer Verlag) pp 365–80

[2] Brandt N, Hirth M, Fichter W, Schubert R, Warren C, Wealthy R 2008, *Experiment Performance Budget*, S2-ASD-TN-3036, Issue 2.2, LISA Pathfinder Project Documentation

[3] Fichter W, Schleicher A, Schlotterer M, Saage R 2008, *DFACS General Design*, S2-ASD-TN-3001, Issue 3, LISA Pathfinder Project Documentation

[4] Schleicher A, Brandt N, Hirth M, Saage R and Fichter W 2008, *Drag-free control design for misaligned cubic test masses, Proc. of the 7th ESA Conf. on Guidance, Navigation and Control Systems*, unpublished

[5] Wanner G 2008, *LTP-OBI Alignment Simulation*, S2-AEI-TN-3051, Issue 2, LISA Pathfinder Project Documentation